

# Imaging of Intra-articular Masses<sup>1</sup>

## CME FEATURE

See accompanying test at [http://www.rsna.org/education/rg\\_cme.html](http://www.rsna.org/education/rg_cme.html)

## LEARNING OBJECTIVES FOR TEST 4

After reading this article and taking the test, the reader will be able to:

- Understand simple and complex joint anatomy to localize masses confidently within the articular space.
- Describe a variety of intraarticular masses.
- Recognize the typical imaging features of intraarticular masses.

Patrick J. Sheldon, MD • Deborah M. Forrester, MD • Thomas J. Learch, MD

Intraarticular masses can be classified as noninfectious synovial proliferative processes (lipoma arborescens, synovial osteochondromatosis, pigmented villonodular synovitis, rheumatoid arthritis), infectious granulomatous diseases (tuberculous arthritis, coccidioidomycosis arthritis), deposition diseases (gout, amyloid arthropathy), vascular malformations (synovial hemangioma, arteriovenous malformations), malignancies (synovial chondrosarcoma, synovial sarcoma, synovial metastases), and miscellaneous (cyclops lesion). Knowledge of articular anatomy aids the radiologist in localizing masses to the joint space. Some joints have complex anatomy with contiguous or adjacent bursae, recesses, and tendinous connections from which masses may originate or into which masses may extend. Many of the diseases causing intraarticular masses have specific imaging characteristics, especially on magnetic resonance images, and knowledge of these characteristics will allow for a more confident diagnosis.

©RSNA, 2005

**Abbreviations:** AVM = arteriovenous malformation, PVNS = pigmented villonodular synovitis, STIR = short inversion time inversion recovery

RadioGraphics 2005; 25:105-119 • Published online 10.1148/rg.251045050 • Content Code: **MK**

<sup>1</sup>From the Department of Radiology, University of Southern California Keck School of Medicine, 1200 N State St, Suite 3550, Los Angeles, CA 90033. Presented as an education exhibit at the 2003 RSNA Scientific Assembly. Received March 23, 2004; revision requested April 27 and received June 1; accepted June 1. All authors have no financial relationships to disclose. Address correspondence to P.J.S. (e-mail: [psheldon@usc.edu](mailto:psheldon@usc.edu)).

©RSNA, 2005



**a.**  
**Figure 1.** (a) Arthrogram of the right shoulder in a patient with calcific bursitis reveals a calcified nodule in the subdeltoid bursa (white arrowhead). Note the normal extension of contrast material into the axillary recess (black arrowhead), into the subscapular bursa (black arrow), and along the tendon sheath of the long head of the biceps brachii muscle (white arrow). (b) Anteroposterior radiograph of the right shoulder in a different patient with synovial osteochondromatosis shows the characteristic calcified nodules. Understanding of the normal joint anatomy is essential to realize that the calcified nodules are intra-articular in the axillary recess (arrowhead), in the subscapular bursa (black arrow), and extending along the biceps tendon sheath (white arrow).

## Introduction

The differential diagnosis for intraarticular masses is a limited one. Knowledge of articular and bursal anatomy aids the radiologist in localizing masses to the joint space and helps in the exclusion of soft-tissue sarcomas from the differential diagnosis.

Intraarticular masses can be classified as **non-infectious synovial proliferative processes** (lipoma *arborescens*, synovial *osteochondromatosis*, pigmented villonodular synovitis [PVNS], *rheumatoid arthritis*), **infectious granulomatous diseases** (*tuberculous arthritis*, *coccidioidomycosis arthritis*), **deposition diseases** (*gout*, *amyloid arthropathy*), **vascular malformations** (synovial *hemangioma*, arteriovenous malformations [AVMs]), **malignancies** (synovial *chondrosarcoma*, synovial sarcoma, synovial metastases), and **miscellaneous conditions** (*cyclops lesion*). Many of the diseases causing intraarticular masses have specific imaging characteristics, especially on magnetic resonance (MR) images, that allow for a confident diagnosis. This article reviews simple and complex joint anatomy, describes a variety of intraar-

ticular masses, and presents their typical imaging findings.

## Joint Anatomy

Knowledge of articular anatomy aids the radiologist in localizing masses to the joint space. This knowledge is particularly helpful for the diagnosis of intraarticular masses in complex joints.

The simple diarthrodial joint consists of cartilage covering the articular ends of the bones forming the joint, an articular capsule formed by ligamentous structures, and a joint space lined with synovial membrane and filled with synovial fluid. Of note, the synovial membrane lines all structures except the articular cartilage. In these simple joints, identifying intraarticular masses is not a challenge.

Several other joints (such as the shoulder, hip, and knee), however, have more complex anatomy, with contiguous or adjacent bursae, recesses, and tendinous connections from which masses may originate or into which masses may extend (Figs 1, 2).

Although separate from the elbow joint space, the olecranon bursa is lined with synovial membrane and can be the site of masses that arise from the synovium. In patients with gout, for example,

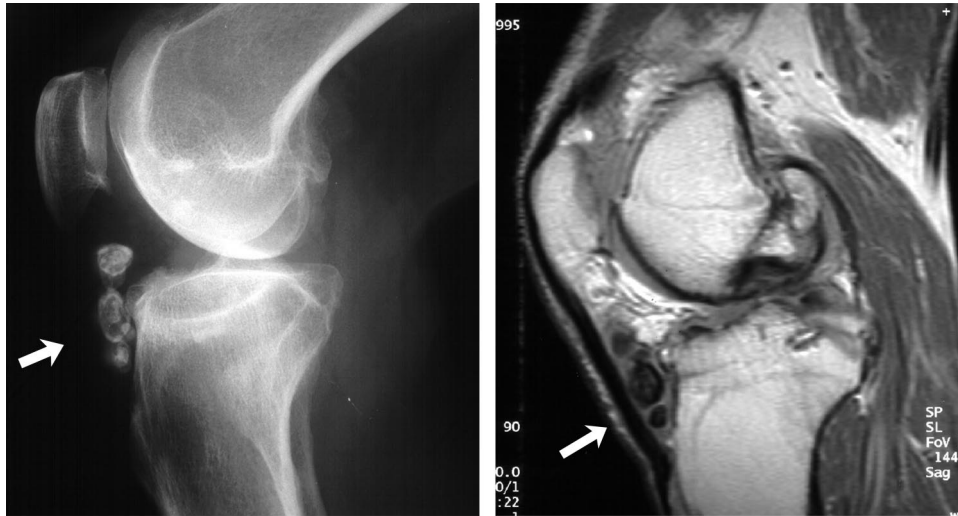


**Figure 2.** Synovial osteochondromatosis of the right knee in a 42-year-old patient. (a) Lateral radiograph shows multiple calcified nodules (arrow) anterior to the proximal tibia. (b) Sagittal proton density-weighted MR image demonstrates that these low-signal-intensity calcified nodules (arrow) are located in the deep infrapatellar bursa.

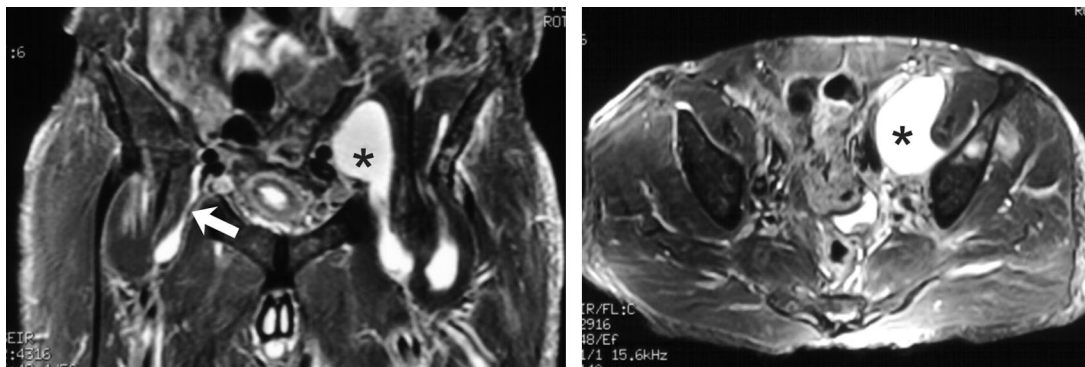


**Figure 3.** Coronal (a) and axial (b) short inversion time inversion-recovery (STIR) images demonstrate bilateral hip joint effusions, with the left effusion being larger than the right. The left hip effusion fills a distended left iliopsoas bursa (\*), and the small right hip joint effusion extends into the right iliopsoas bursa (arrow).

the olecranon bursa can contain tophaceous deposits that appear on conventional radiographs as a characteristic cloudlike area of increased opacity posterior to the olecranon.

Connection of the hip joint to the [iliopsoas bursa](#) is found in 15% of the population (1). This connection can allow a hip joint effusion to distend the iliopsoas bursa (Fig 3). Distention of the iliopsoas bursa from intraarticular disease may produce a mass in the ilioinguinal region that can

simulate a hernia and cause obstruction of the femoral vein (2).

Similarly, a [normal connection](#) between the [ankle joint and the flexor hallucis longus tendon sheath](#) is seen in approximately 20% of the population (3). In patients with septic arthritis of the ankle, this connection can provide a direct path for infection to spread into the calf (Fig 4).

**Figure 4.** Septic arthritis of the ankle joint. (a) Anteroposterior arthrogram demonstrates contrast material extending up the calf (arrow). Note the sinus track exiting out to the skin laterally (arrowhead). (b) Sagittal STIR MR image demonstrates fluid extending up from the ankle joint into the flexor hallucis longus tendon sheath (arrow).

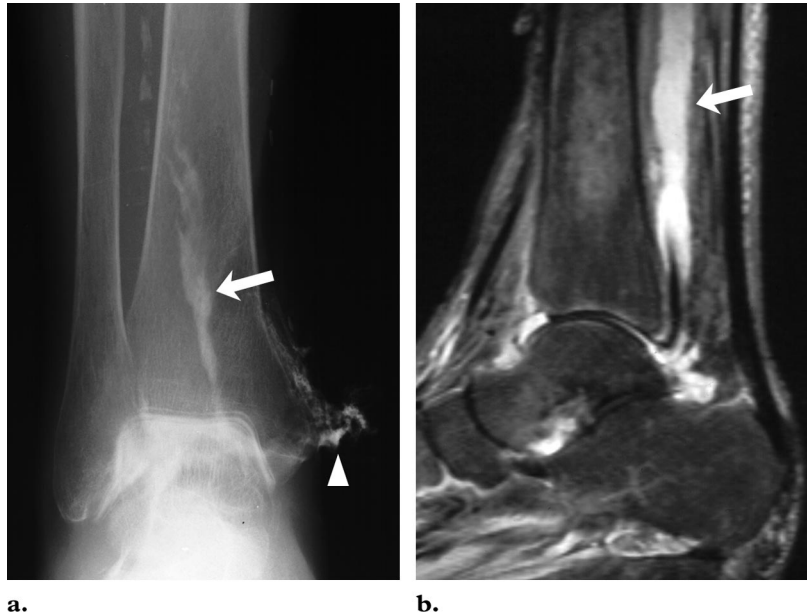


**Figure 5.** Lipoma arborescens in a 50-year-old man with knee swelling.

(a) Lateral radiograph of the knee reveals fullness of the suprapatellar bursa with radiolucent areas (arrow) suggestive of fat. (b) Sagittal proton density-weighted MR image shows a lobulated mass in the suprapatellar bursa (arrow) with signal intensity equivalent to that of fat. (c) Sagittal proton density-weighted MR image with fat saturation shows loss of signal of the synovial proliferation (arrow) surrounded by a large joint effusion extending into the popliteal bursa (\*). (d) Long-axis ultrasound (US) image shows distention of the suprapatellar bursa by a mass with characteristic frond-like projections (arrows) surrounded by a joint effusion (\*).



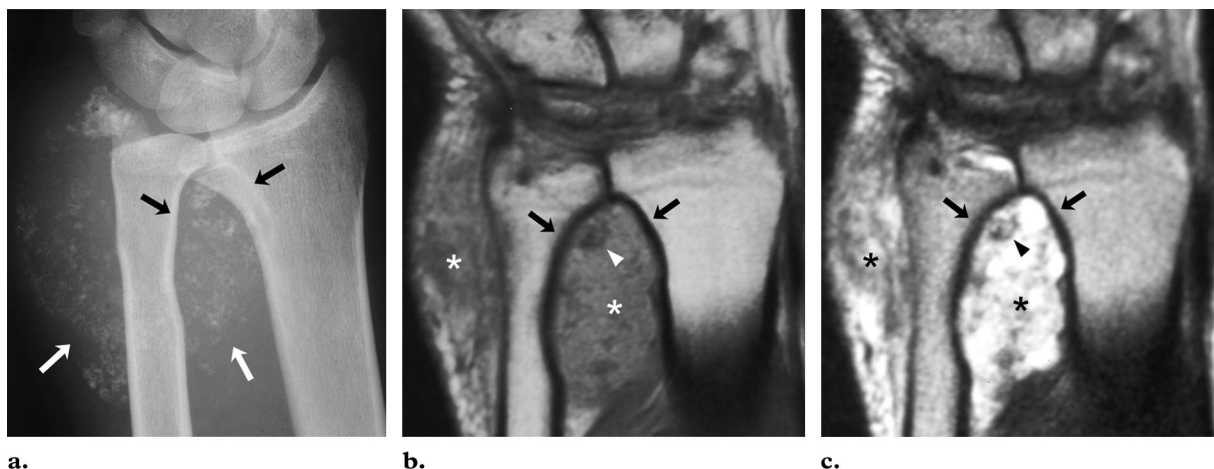


**Figure 6.** Synovial osteochondromatosis of the wrist. **(a)** Anteroposterior radiograph of the wrist demonstrates multiple small, calcified nodules (white arrows) of characteristically uniform size in the radioulnar joint. Note the erosive changes (black arrows) of the distal radius and ulna. **(b)** Coronal proton density-weighted MR image demonstrates an intermediate-signal-intensity mass (\*) in the radioulnar joint. **(c)** Coronal T2-weighted image shows that the mass (\*) is hyperintense. On both MR images, note the multiple low-signal-intensity areas (arrowhead), which correspond to areas of calcification seen on the radiograph.

## Noninfectious Synovial Proliferative Processes

### Lipoma Arborescens

Lipoma arborescens is a rare intraarticular lesion characterized by the replacement of the subsynovial tissue by mature fat cells, giving rise to a villous synovial proliferation. Lipoma arborescens is usually monarticular and occurs most frequently in the knee, particularly in the suprapatellar pouch. Most patients are in the 5th to 7th decades of life. Affected patients usually report a long-standing, painless, slowly progressive swelling of the joint with recurrent effusions (4). The exact cause is unknown, but the most accepted hypothesis suggests that lipoma arborescens represents a nonspecific synovial reaction to inflammatory or traumatic stimuli rather than a neoplasm (5). Synovectomy is the definitive treatment. Postoperative recurrence is uncommon.

Lipoma arborescens has many characteristic imaging findings that allow for a confident diagnosis (Fig 5). Radiographs typically show joint fullness and, frequently, osteoarthritic changes. These findings are nonspecific, and the diagnosis can be suspected only when radiolucent areas suggestive of fat are seen in a joint space. US demonstrates a hyperechoic, frondlike mass that bends and waves in real time during joint manipulation (6). The characteristic subsynovial hypertrophic adipose proliferation allows for a precise diagnosis with MR imaging, especially when T1-weighted and fat-suppressed sequences are used, since the lesion has fat signal intensity with all pulse sequences.

### Synovial Osteochondromatosis

Synovial osteochondromatosis is a benign monarticular disorder of uncertain cause characterized by proliferation and metaplastic transformation of the synovium with formation of multiple cartilaginous nodules. It is twice as common in men and usually occurs in the 3rd to 5th decades of life. The knee is the most commonly affected joint, followed by the elbow, hip, and shoulder. Synovial osteochondromatosis manifests clinically with joint pain, swelling, and limitation of motion (7).

The disease progresses from an active initial phase, with synovial proliferation and formation of intrasynovial cartilaginous nodules, to a final phase, which is characterized by inactive synovial disease and persistent nodules, which may break off into the joint space. The nodules may contain unmineralized cartilage alone (synovial chondromatosis), cartilage and bone, or mature bone with fatty marrow. Calcification is absent in approximately 25%–30% of patients (8). Treatment is surgical synovectomy; however, the recurrence rate is over 25% (8).

When calcified bodies are present, the radiographic findings of synovial osteochondromatosis are pathognomonic, consisting of multiple intraarticular calcified nodules, characteristically uniform in size (Fig 6a). Synovial osteochondromatosis may be associated with a small joint effusion, marginal erosions, and late secondary degenerative joint disease. The MR imaging appearance is variable and depends on the relative proportion of synovial proliferation and calcified nodule formation. Nonmineralized lesions tend to form an

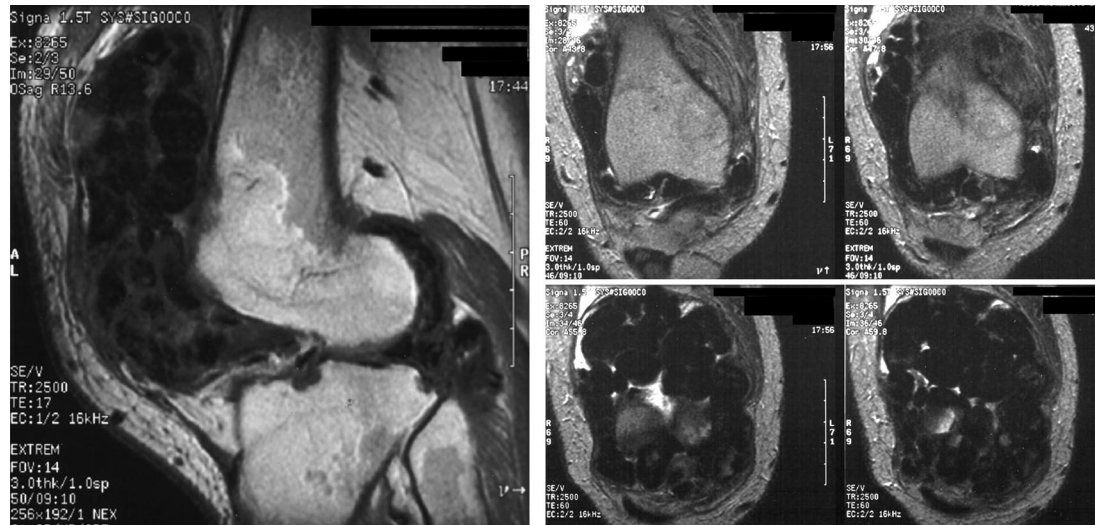


**Figure 7.** Diffuse PVNS of the knee in a 43-year-old woman. **(a)** Sagittal proton density-weighted MR image shows lobulated, masslike synovial proliferation with characteristic low signal intensity. Note the tibial articular erosions. **(b)** Corresponding coronal T2-weighted MR images through the anterior right knee demonstrate massive distention of the suprapatellar pouch by lobulated proliferative synovium with characteristic low signal intensity because of hemosiderin deposition.

intraarticular conglomerate mass that is isointense relative to muscle on T1-weighted images and hyperintense on T2-weighted images (Fig 6b, 6c). When the cartilaginous nodules contain calcification, small areas of low signal intensity are observed with all pulse sequences. Intraarticular bodies with mature bone and fatty marrow display low signal intensity of cortical bone peripherally and high signal intensity of bone marrow fat centrally on T1-weighted images (9).

### Pigmented Villonodular Synovitis

PVNS is a benign proliferative disorder of the synovium that may affect the joints, bursae, or tendon sheaths. It can appear in either a diffuse (Fig 7) or, less commonly, a focal (Fig 8) form within the joint (10).

PVNS most often occurs in young to middle-aged adults. The knee is the most frequently involved joint, followed by the hip, ankle, and shoulder (11). Local recurrence following surgical or arthroscopic synovectomy occurs in almost 50% of cases (8). Polyarticular involvement is extremely rare.

Conventional radiographs of joints affected by PVNS may appear normal or may demonstrate periarticular soft-tissue swelling. Joint spaces and bone mineralization are characteristically preserved until late in the disease. Bone erosions are common in joints with a tight capsule, such as the

hip and ankle. On MR images, the masslike proliferative synovium has a lobulated margin, and it may be extensive in diffuse PVNS or limited to a single nodule in the focal form. The lesions tend to bleed, causing hemosiderin deposition and a characteristic low signal intensity with all pulse sequences (12). Areas of high signal intensity on T2-weighted images may be present and are likely caused by inflamed synovium or joint effusions (9).

### Rheumatoid Arthritis

Rheumatoid arthritis is a chronic systemic disorder that primarily involves the joints and affects 1% of the population worldwide (13). Women are more commonly affected than men, and most patients present between the 4th and 6th decades of life. Rheumatoid arthritis most commonly affects the hands, wrists, and feet (13).

Although the pathogenesis of rheumatoid arthritis is unknown, it is believed that cross-reacting antibodies to an unknown antigen are deposited in the synovium, leading to invasion by neutrophils and macrophages. This inflammatory response results in a proliferative, hyperplastic, and hypervascular synovium called *pannus* (14).

On conventional radiographs, joints affected with rheumatoid arthritis have soft-tissue swelling, marginal erosions, periarticular osteopenia, and diffuse joint space loss. MR imaging demonstrates intermediate- to low-signal-intensity pannus on T1- and T2-weighted images in the affected joints (Fig 9) (15).

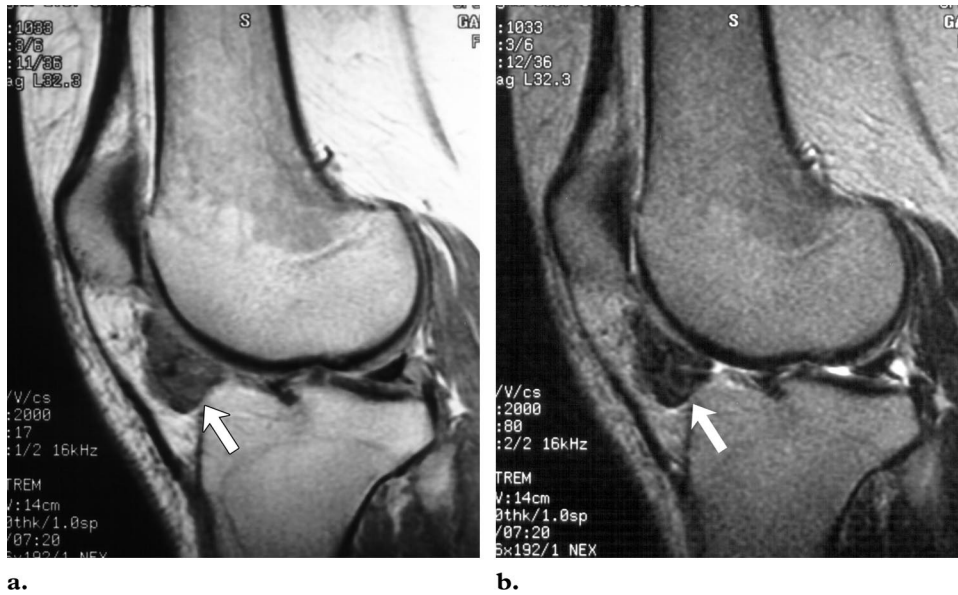


**Figure 8.** Focal PVNS of the knee in a 47-year-old woman. (a) Sagittal proton density-weighted MR image demonstrates a low-signal-intensity mass (arrow) in the anterior joint space. (b) Sagittal T2-weighted MR image shows the mass (arrow) with characteristic persistent low signal intensity.

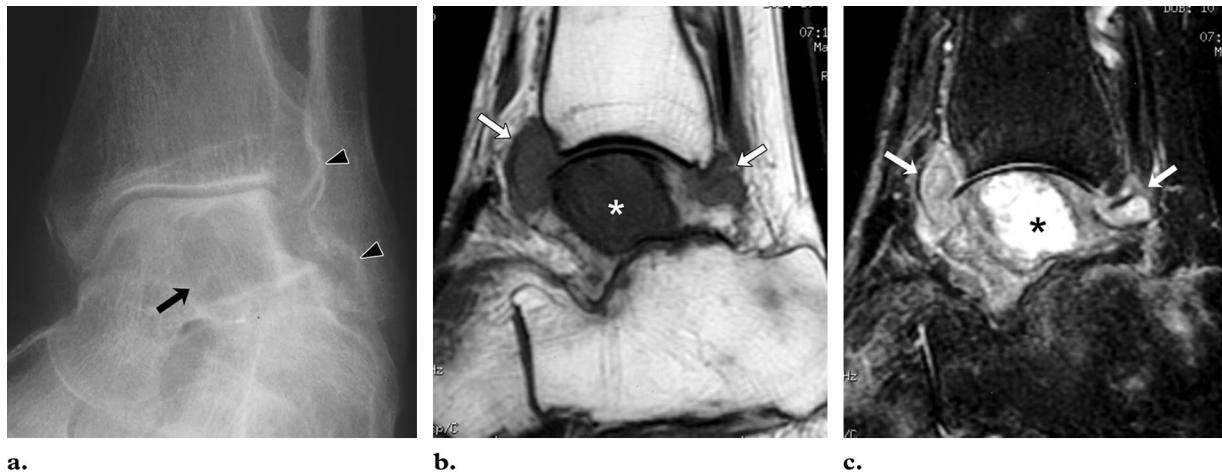


**Figure 9.** Rheumatoid arthritis of the ankle in a 61-year-old woman. (a) Anteroposterior radiograph of the ankle demonstrates a large lytic lesion in the talus (arrow). The lesion was initially thought to be a bone tumor, but the erosions of the fibula (arrowheads) indicate that the primary disease is in the joint. (b) Sagittal T1-weighted MR image demonstrates a low-signal-intensity lesion (\*) in the talus with low-signal-intensity pannus (arrows) in the joint space. (c) Sagittal STIR MR image demonstrates intermediate-signal-intensity pannus (arrows) and high signal intensity in the talus representing a large subchondral geode (\*).

## Infectious Granulomatous Diseases

### Tuberculous Arthritis

Musculoskeletal manifestations occur in approximately 3% of patients with tuberculosis, with about half of these cases manifesting as spondylitis or Pott disease (16). The remaining musculoskeletal tuberculous infections consist of tenosynovitis, bursitis, and arthritis (17).

Tuberculous arthritis most commonly occurs in the hip and knee (16). In our experience, tuberculous arthritis results from the hematogenous spread of an active pulmonary or lymphatic focus of tuberculosis to the synovium; in rare cases,

direct spread from an adjacent focus of osteomyelitis can occur.

Radiographic findings suggestive of tuberculous arthritis include monarticular involvement, soft-tissue swelling, joint effusions, periarticular osteopenia, and marginal erosions. Joint space narrowing is unusual because the articular cartilage is typically preserved until late in the disease (18). Computed tomography (CT) and MR imaging are helpful in detecting and characterizing the periarticular abscesses often found in tuberculous arthritis (Fig 10) (19).

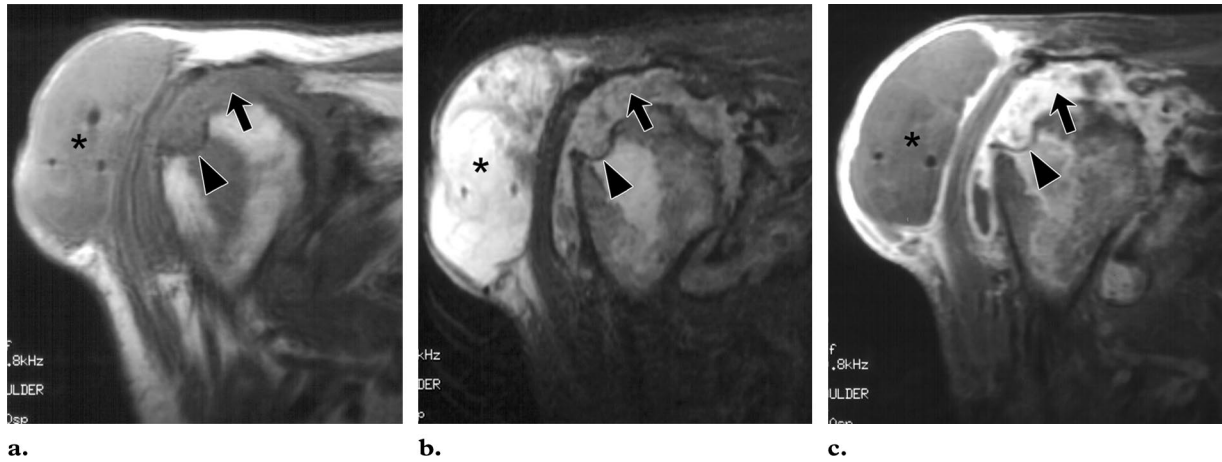


**Figure 10.** Tuberculous arthritis of the right shoulder in a patient with clinically suspected sarcoma because of a large rock-hard mass in the shoulder. **(a, b)** Coronal T1-weighted MR image **(a)** and T2-weighted image with fat saturation **(b)** of the right shoulder demonstrate a humeral head erosion (arrowhead) and a distended joint space with proliferative synovium (arrow). Note the adjacent large mass (\*). **(c)** Coronal postcontrast T1-weighted MR image with fat saturation demonstrates that the mass (\*) is a fluid-filled collection with an enhancing periphery rather than a solid tumor. Note the enhancement of the synovium within the joint (arrow) and the marginal erosion (arrowhead). The combination of a destructive inflammatory arthritis decompressing into the adjacent subdeltoid bursa to form a cold abscess is typical of tuberculous arthritis.



**Figure 11.** Coccidioidomycosis arthritis of the knee. **(a, b)** Coronal T1-weighted MR image **(a)** and proton density-weighted MR image with fat saturation **(b)** demonstrate a joint effusion and marginal erosions of the proximal tibia with preservation of the joint spaces. **(c)** Axial proton density-weighted MR image with fat saturation demonstrates multiple rice bodies (arrow) within a joint effusion.

### Coccidioidomycosis Arthritis

Coccidioidomycosis results from inhalation of the fungus *Coccidioides immitis* in endemic areas of Mexico, South America, and the southwestern United States. In some persons, disseminated disease may develop with spread of infection to the liver, spleen, lymph nodes, and bones.

Joint involvement by coccidioidomycosis arthritis usually occurs in the ankle and knee. Monoarticular arthritis is most common. In general, articular infections result from direct extension of

an osteomyelitis focus; direct hematogenous spread to a joint can occur in rare cases (20).

Radiographic findings of coccidioidomycosis arthritis are similar to those observed in other granulomatous articular infections: juxtaarticular osteopenia, joint effusions, and relatively preserved joint spaces until late in the course of the disease (Fig 11) (21). As with rheumatoid arthritis and tuberculous arthritis, coccidioidomycosis arthritis can result in synovial rice bodies (Fig 11c), which are detached synovial villi lying within the joint cavity that resemble grains of rice and contain coarse collagenous fibers, reticulin, and elastin (22).





**a.** **b.**  
**Figure 12.** Gout in a 48-year-old man with suspected osteomyelitis of the first toe. **(a)** Sagittal T1-weighted MR image of the first toe demonstrates an erosion with an overhanging edge (arrow) at the distal metatarsal head, preserved joint space, and a periarticular intermediate-signal-intensity gouty tophus (\*). **(b)** Sagittal STIR MR image demonstrates low signal intensity of the gouty tophus (\*).

## Deposition Diseases

### Gout

Gout is a metabolic disorder characterized by hyperuricemia that arises from either an increase in production or a decrease in excretion of uric acid. Chronic hyperuricemia results in deposition of sodium monourate within or around the joints. Tophaceous gout is characterized by the presence of tophi, local aggregates of urate crystals and proteinaceous matrix surrounded by an intense inflammatory reaction. Chronic tophaceous gout occurs much more frequently in men and usually is seen in the 5th to 7th decades of life. The most common locations for tophi include the joints of the hands and feet (8).

Characteristic radiographic findings of gout include well-defined erosions with overhanging edges, preservation of joint spaces, lack of periarticular osteopenia, and soft-tissue nodules. The lesions usually have intermediate signal intensity on T1-weighted MR images and intermediate to low signal intensity on T2-weighted MR images (Fig 12) (23).

Several inherited enzymatic defects have been identified as causing hyperuricemia, leading to gout. Kelley-Seegmiller syndrome results from partial hypoxanthine-guanine phosphoribosyltransferase (HPRT) deficiency, which leads to the onset of gout in late childhood. Up to 25% of patients with Kelley-Seegmiller syndrome may have minor neurologic features, but these children do not exhibit self-mutilating biting, in contrast to those with Lesch-Nyhan syndrome in which HPRT deficiency is complete (24).

### Amyloid Arthropathy

Amyloid arthropathy is characterized by the accumulation of amyloid in and around the joints. There are a large number of unrelated proteins that can constitute an amyloid fibril, including immunoglobulin light chains,  $\beta_2$ -microglobulin, serum amyloid A, and calcitonin.

Amyloid arthropathy is most commonly seen in patients undergoing chronic hemodialysis (and is caused by elevated serum levels of  $\beta_2$ -microglobulin) and in patients with plasma cell dyscrasia (in these patients, amyloid arthropathy is caused by elevated serum levels of monoclonal immunoglobulin light chain fragments) (25). Less commonly, amyloid arthropathy can be seen in patients with chronic inflammatory diseases such as rheumatoid arthritis, familial Mediterranean fever, and chronic osteomyelitis (caused by chronically elevated serum levels of an acute-phase protein, serum amyloid A) (26).

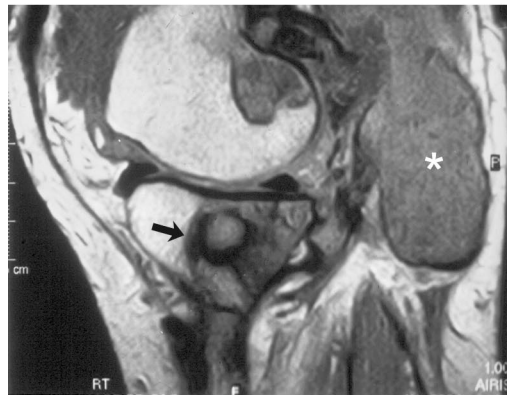
The articular changes of amyloid arthropathy are bilateral and most frequently affect the shoulders, hips, knees, and wrists (27). Amyloid spondyloarthropathy occurs predominantly, but not exclusively, in dialysis patients (25).

Characteristic findings of amyloid arthropathy on conventional radiographs and CT scans include juxtaarticular soft-tissue masses, periarticular osteopenia, subchondral cysts, joint effusions, erosions, and preserved joint spaces (25). On MR images, amyloid deposits are characterized by low to intermediate signal intensity regardless of pulse sequence (Fig 13) (28). The lesions exhibit no

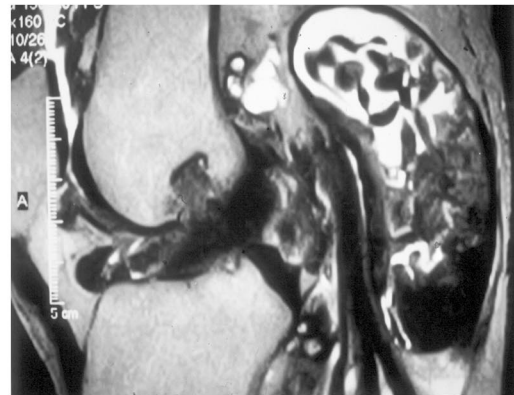
**Figure 13.** Amyloid arthropathy in a 70-year-old woman with a 15-year history of dialysis. **(a)** Anteroposterior radiograph of the knee demonstrates a lytic lesion of the medial posterior tibia (arrow). **(b)** Sagittal T1-weighted MR image reveals distention of the joint space and popliteal cyst (\*) by intermediate-signal-intensity material with a pressure erosion of the posterior tibia (arrow). **(c)** Sagittal T2-weighted MR image demonstrates fluid as well as low-signal-intensity amyloid deposits filling the joint space and popliteal cyst. (Case reprinted, with permission, from reference 28.)



a.



b.



c.



a.



b.



c.

**Figure 14.** Synovial hemangioma in a 21-year-old woman who complained of a mass above her knee. **(a)** Sagittal proton density-weighted MR image of the knee shows an intermediate-signal-intensity mass (arrow) in the suprapatellar bursa that invades the musculature anteriorly. **(b)** Sagittal proton density-weighted MR image with fat saturation demonstrates the markedly high signal intensity of this synovial hemangioma, a finding that reflects pooling of blood within vascular spaces. **(c)** Axial proton density-weighted MR image with fat saturation demonstrates the high-signal-intensity mass in the suprapatellar bursa that extends anteriorly into the vastus medialis muscle (arrow).

paramagnetic effect on gradient-echo MR images, a finding that is helpful in differentiating amyloid arthropathy from synovial conditions characterized by hemosiderin deposition (eg, PVNS) (9).

## Vascular Malformations

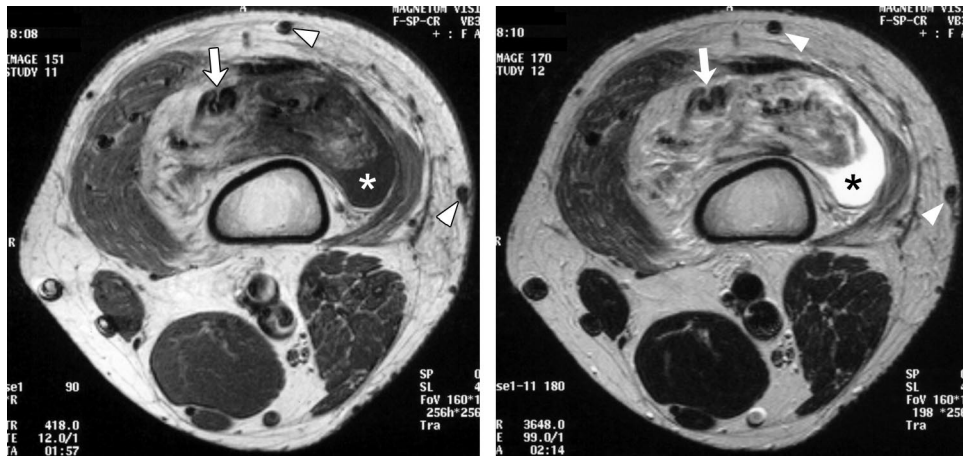
### Synovial Hemangioma

Synovial hemangioma is a rare benign vascular malformation that usually affects children and young adults and occurs predominantly in the



**Figure 15.** Klippel-Trénaunay-Weber syndrome in a 25-year-old man. **(a)** Photograph shows a nevus flammeus (arrow) of the left lower extremity. Note the overgrowth of the left leg and foot. **(b, c)** Axial T1-weighted **(b)** and T2-weighted **(c)** MR images demonstrate a joint effusion (\*) and an intermediate-signal-intensity AVM in the suprapatellar bursa with a prominent serpentine signal void (arrow) from a large feeding artery. Note the large superficial dilated veins (arrowheads).

**a.**



**b.**

**c.**

knee. Patients usually present with joint pain, swelling, and spontaneous hemarthrosis (29).

Conventional radiographs of a patient with synovial hemangioma often demonstrate a non-specific soft-tissue mass. Phleboliths are not uncommon. MR imaging findings of synovial hemangioma are frequently pathognomonic, consisting of a lobulated intraarticular mass with characteristic signal intensity. The mass usually has intermediate signal intensity on T1-weighted images, and its marked hyperintensity on T2-weighted images likely reflects pooling of blood within vascular spaces (Fig 14). Low-signal-intensity linear structures seen throughout the lesion on T2-weighted images are believed to represent fibrous septa or vascular channels (30).

MR imaging is especially useful in planning surgical treatment for synovial hemangioma, since it demonstrates the exact location and extent of the tumor. Pedunculated and well-circumscribed masses can be resected arthroscopically, whereas diffuse lesions require open excision. Recurrence is common in cases of diffuse synovial hemangioma (31).

### Arteriovenous Malformations

AVMs are characterized by an abnormal connection between arteries and veins. Arterial blood is shunted to the venous system in a central confluence of tortuous vessels, called a nidus. Although AVMs are congenital, they are often not discovered until later in life.

Extremity AVMs are relatively common. They may be single or multifocal in the extremity, or they may be diffuse and involve the entire extremity and adjacent trunk (32). Although they are less common than extremity AVMs, intraarticular AVMs can usually be diagnosed with multiple imaging modalities, which demonstrate a hypervascular lesion with a large feeding arterial vessel.

Klippel-Trénaunay-Weber syndrome is a rare congenital abnormality characterized by cutaneous hemangiomas (nevus flammeus), hypertrophy of bone and soft tissue, varicose veins, and AVMs, usually affecting a single limb (Fig 15) (33). The cause of this syndrome is unknown, but it has been hypothesized that it may be related to

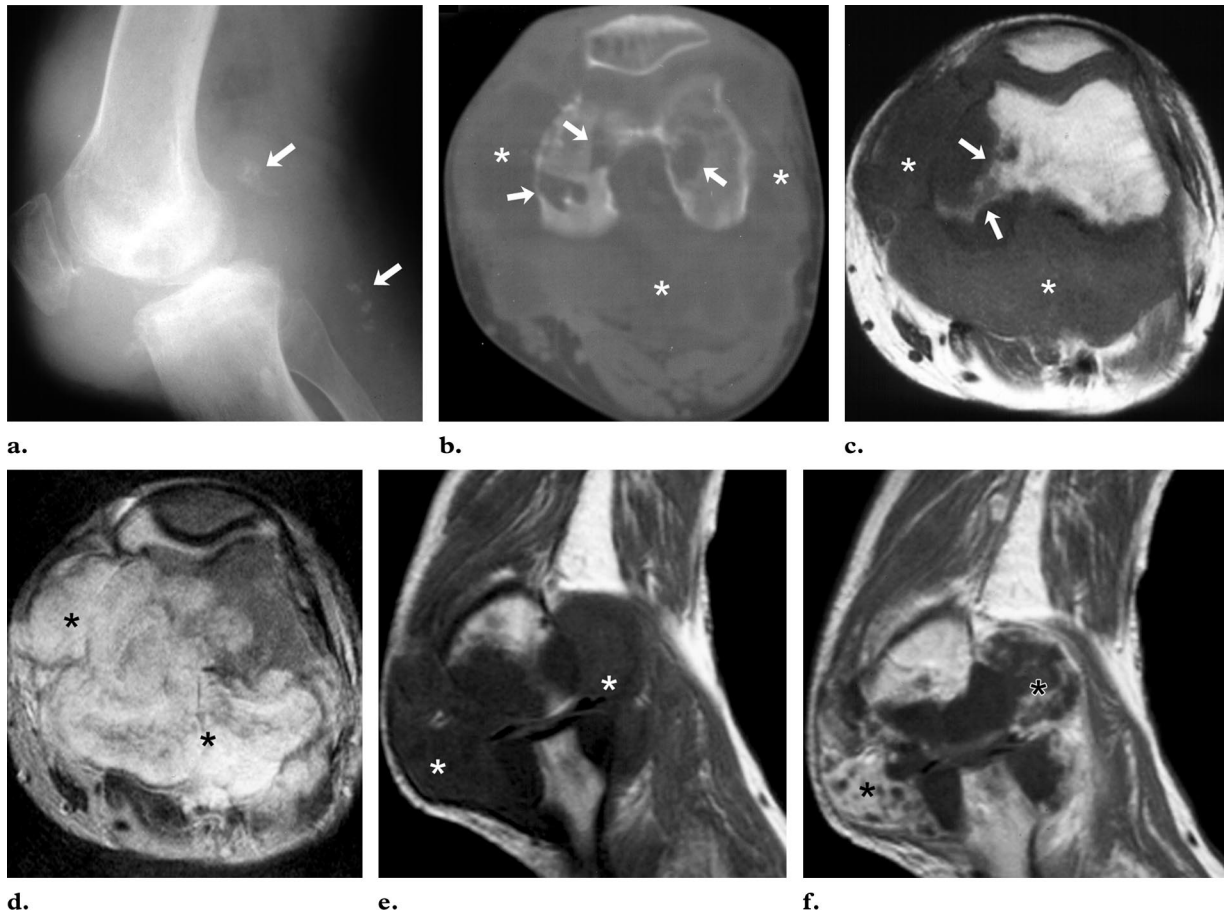


**Figure 16.** Synovial chondrosarcoma in a 52-year-old man with a swollen knee in whom synovial osteochondromatosis had been diagnosed at biopsy 10 years earlier. **(a)** Lateral radiograph of the knee demonstrates distention of the joint space by a soft-tissue mass that contains areas of calcified matrix (arrows). **(b)** Axial CT scan of the knee demonstrates a large soft-tissue mass (\*) in the joint space. Note the erosions of the distal femoral condyles (arrows), which are less apparent on the conventional radiograph. **(c)** Axial T1-weighted MR image demonstrates a large lobulated low-signal-intensity mass (\*) distending the joint space, with erosion and invasion of the femoral condyles (arrows). **(d)** Axial T2-weighted MR image obtained more distally demonstrates high signal intensity (\*) within the mass. **(e, f)** Precontrast **(e)** and postcontrast **(f)** sagittal T1-weighted MR images of the knee demonstrate heterogeneous enhancement of the infiltrating intraarticular synovial chondrosarcoma (\*).

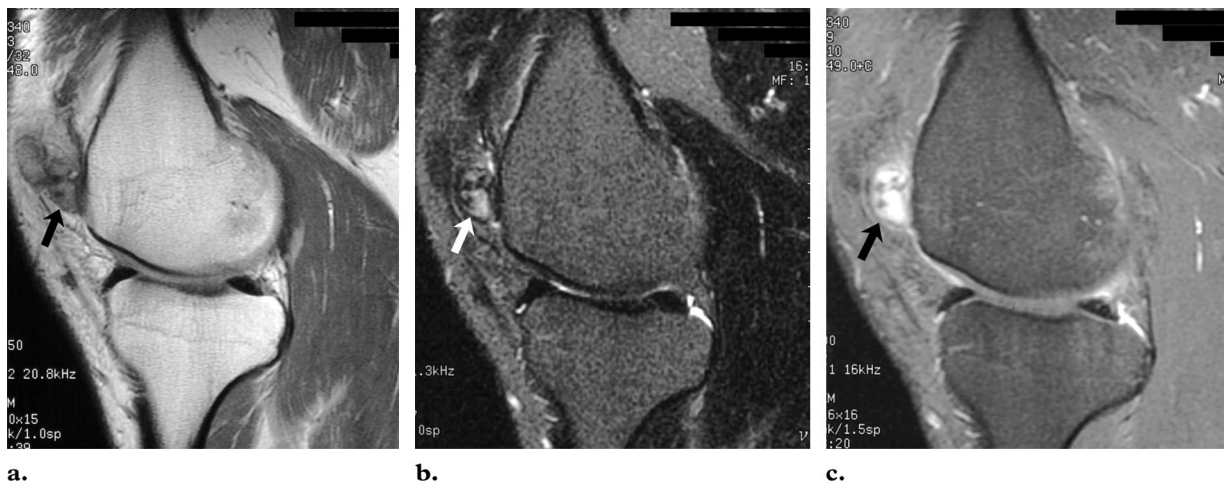


**Figure 17.** Intraarticular synovial sarcoma in a 25-year-old man. **(a)** Sagittal proton density-weighted MR image demonstrates an intermediate-signal-intensity mass (arrow) in the anterior joint space. **(b)** Sagittal T2-weighted MR image with fat saturation demonstrates that the mass has high signal intensity (arrow). **(c)** Sagittal postcontrast T1-weighted MR image with fat saturation demonstrates enhancement of the mass (arrow). Note the foci of persistent low signal intensity with all pulse sequences, an appearance consistent with areas of calcification.

an intrauterine insult during vascular differentiation and invasion of the developing limb bud. The disease is present at birth, but it may be subtle enough to go undetected. Patients usually present in childhood with a unilateral deformed lower extremity.

## Malignancies

### Synovial Chondrosarcoma

Synovial chondrosarcoma is extremely rare. It is not clear whether it arises *de novo* or from malignant degeneration of synovial osteochondromatosis. Like synovial osteochondromatosis, synovial chondrosarcoma is characterized by metaplastic transformation of the synovium with formation of multiple cartilaginous nodules that can calcify and ossify. It affects patients between the 4th and 7th decades of life and most commonly involves the knee and hip. Distant metastases usually appear in the lungs (34).

The radiologic differentiation of synovial chondrosarcoma from synovial osteochondromatosis is difficult. Conventional radiographs usually demonstrate an intraarticular soft-tissue mass, which may contain calcified bodies (Fig 16a). On T1-weighted MR images, synovial chondrosarcoma is often lobulated, with isointense signal; it has hyperintense signal on T2-weighted images (Fig 16). When the associated cartilaginous nodules contain calcification, small areas of low signal intensity are observed with all pulse sequences. Bone erosions can be seen in both synovial osteochondromatosis and synovial chondrosarcoma (35).

### Synovial Sarcoma

Synovial sarcoma is a mesenchymal neoplasm that accounts for 10% of all primary soft-tissue malignant tumors (36). Most synovial sarcomas are located in the extremities, with two-thirds being in the lower extremities, particularly around the knee. Synovial sarcoma is so named because of its resemblance to synovial tissue at light microscopy. Despite its name, synovial sarcoma does not arise from the synovial membrane but rather from primitive mesenchymal cells in the extraarticular soft tissues. Fewer than 5% of synovial sarcomas arise within the joint space (37).

Radiographs may demonstrate calcification in 20%–30% of synovial sarcomas (37). These le-

sions usually demonstrate low signal intensity on T1-weighted MR images and high signal intensity on T2-weighted images (Fig 17). Cystic areas, areas of hemorrhage, and fluid-fluid levels are often seen (36).

### Synovial Metastases

The metastatic spread of tumors to the joints and synovium is a rare manifestation of malignant disease, despite the highly vascular nature of the synovium. Of tumors metastasizing to the synovium, primary lung cancers do so most frequently (38).

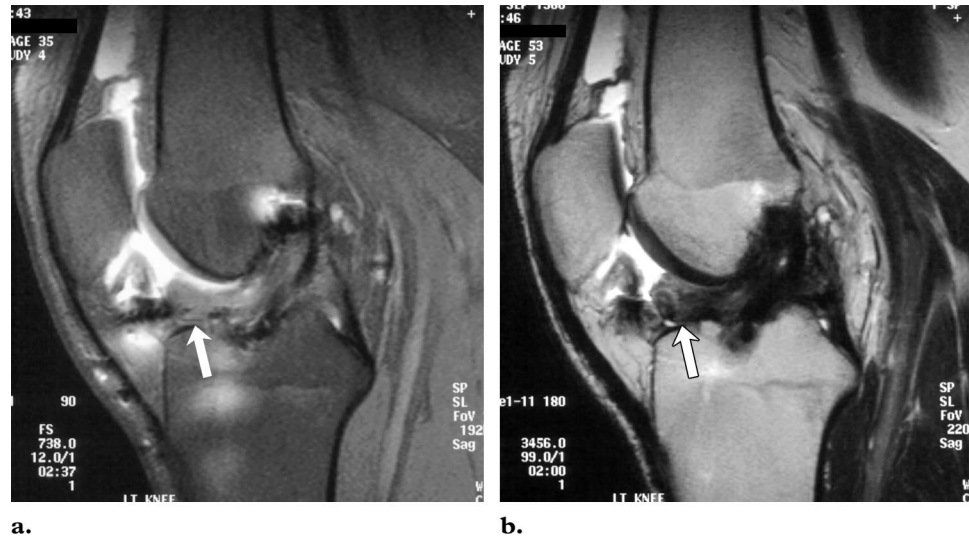
Metastatic arthritis can involve the synovium, the joint cartilage, or both. The knee is most commonly affected. Diagnosis can be made with either cytologic examination of the synovial fluid or synovial biopsy. Prognosis is generally poor, with an average survival of less than 5 months (38).

### Miscellaneous Lesions: Cyclops Lesion

The cyclops lesion occurs with an estimated frequency of 1%–9.8% following anterior cruciate ligament reconstruction (39). Although the precise cause is unknown, it is believed that uplifting of fibrocartilaginous tissue during drilling of the tibia for anterior cruciate ligament reconstruction serves as a nidus for fibrous tissue deposition. Pathologically, the lesion consists of central granulation tissue surrounded by dense fibrous tissue. The lesion was so named because of its bulbous appearance and characteristic focal areas of reddish-blue discoloration (from venous channels) that resemble an eye at arthroscopy. The lesion may result in loss of full extension. Surgical débridement of the lesion results in restoration of full knee extension (39).

At MR imaging, a soft-tissue mass is seen anteriorly or anterolaterally in the intercondylar notch near the tibial insertion of the reconstructed anterior cruciate ligament. Because of its fibrous content, a cyclops lesion typically has intermediate to low signal intensity with all pulse sequences (Fig 18) (40).

**Figure 18.** Cyclops lesion in a patient after anterior cruciate ligament reconstruction. (a) Sagittal T1-weighted MR image of the knee with fat saturation demonstrates an intermediate-signal-intensity mass anteriorly in the joint space (arrow). (b) Sagittal T2-weighted MR image demonstrates the characteristic low signal intensity of this fibrous mass (arrow).



### Summary

The differential diagnosis for intraarticular masses is limited. Anatomic knowledge aids the radiologist in localizing masses to the joint space. Familiarity with the typical imaging characteristics as described in this article allows one to make confident diagnoses of many of the diseases causing intraarticular masses (Table).

### References

1. Armstrong P, Saxton H. Ilio-psoas bursa. *Br J Radiol* 1972; 45:493–495.
2. Warren R, Kaye JJ, Salvati EA. Arthrographic demonstration of an enlarged iliopsoas bursa complicating osteoarthritis of the hip: a case report. *J Bone Joint Surg Am* 1975; 57:413–415.
3. Olson RW. Arthrography of the ankle: its use in the evaluation of ankle sprains. *Radiology* 1969; 92:1439–1446.
4. Martin S, Hernandez L, Romero J, et al. Diagnostic imaging of lipoma arborescens. *Skeletal Radiol* 1998; 27:325–329.
5. Vilanova JC, Barcelo J, Villalon M, Aldoma J, Delgado E, Zapater I. MR imaging of lipoma arborescens and the associated lesions. *Skeletal Radiol* 2003; 32:504–509.
6. Learch TJ, Braaton M. Lipoma arborescens: high-resolution ultrasonographic findings. *J Ultrasound Med* 2000; 19:385–389.
7. Milgram JW. Synovial osteochondromatosis: a histopathological study of thirty cases. *J Bone Joint Surg Am* 1977; 59:792–801.
8. Llauger J, Palmer J, Roson N, Bague S, Camins A, Cremades R. Nonseptic monoarthritis: imaging features with clinical and histopathologic correlation. *RadioGraphics* 2000; 20:S263–S278.
9. Narvaez JA, Narvaez J, Ortega R, De Lama E, Roca Y, Vidal N. Hypointense synovial lesions on T2-weighted images: differential diagnosis with pathologic correlation. *AJR Am J Roentgenol* 2003; 181:761–769.
10. Llauger J, Palmer J, Roson N, Cremades R, Bague S. Pigmented villonodular synovitis and giant cell tumors of the tendon sheath: radiologic and pathologic features. *AJR Am J Roentgenol* 1999; 172:1087–1091.
11. Goldman AB, DiCarlo EF. Pigmented villonodular synovitis: diagnosis and differential diagnosis. *Radiol Clin North Am* 1988; 26:1327–1347.
12. Dorwart RH, Genant HK, Johnston WH, Morris JM. Pigmented villonodular synovitis of synovial joints: clinical, pathologic, and radiologic features. *AJR Am J Roentgenol* 1984; 143:877–885.
13. Winalski CS, Palmer WE, Rosenthal DI, Weissman BN. Magnetic resonance imaging of rheumatoid arthritis. *Radiol Clin North Am* 1996; 34:243–258.
14. Tehranzadeh J, Ashikyan O, Dascalos J. Magnetic resonance imaging in early detection of rheumatoid arthritis. *Semin Musculoskelet Radiol* 2003; 7:79–94.
15. Imhof H, Nobauer-Huhman IM, Gahleitner A, et al. Pathophysiology and imaging in inflammatory and blastomatous synovial diseases. *Skeletal Radiol* 2002; 31:313–333.
16. Leigh Moore S, Rafii M. Advanced imaging of tuberculosis arthritis. *Semin Musculoskelet Radiol* 2003; 7:143–153.
17. Learch TJ, Hsiao NM. Tuberculous infection of the gracilis muscle and tendon clinically mimicking deep venous thrombosis: sonographic findings. *Skeletal Radiol* 1999; 28:457–459.
18. Watts HG, Lifeso RM. Tuberculosis of bones and joints. *J Bone Joint Surg Am* 1996; 78:288–298.
19. Suh JS, Lee JD, Cho JH, Kim MJ, Han DY, Cho NH. MR imaging of tuberculous arthritis: clinical and experimental studies. *J Magn Reson Imaging* 1996; 6:185–189.
20. Resnick D. Osteomyelitis, septic arthritis, and soft tissue infection: organisms. In: Resnick D, ed. *Differential diagnosis of bone and joint disorders*. 4th ed. Philadelphia, Pa: Saunders, 2002; 2510–2624.
21. McGahan JP, Graves DS, Palmer PE, Stadalnik RC, Dublin AB. Classic and contemporary imaging of coccidioidomycosis. *AJR Am J Roentgenol* 1981; 136:393–404.
22. Sugano I, Nagao T, Tajima Y, et al. Variation among giant rice bodies: report of four cases and their clinicopathological features. *Skeletal Radiol* 2000; 29:525–529.
23. Gentili A. Advanced imaging of gout. *Semin Musculoskelet Radiol* 2003; 7:165–174.
24. Khattak FH, Morris IM, Harris K. Kelley-Seegmiller syndrome: a case report and review of the literature. *Br J Rheumatol* 1998; 37:580–581.

## Imaging Features of Intraarticular Masses

| Type of Lesion                                 | Key Imaging Features  |
|--|---|
| Noninfectious synovial proliferative processes |   |
| Lipoma arborescens                             | Follows fat signal intensity with all MR imaging pulse sequences  |
| Synovial osteochondromatosis                   | Multiple intraarticular calcified nodules, characteristically uniform in size   |
| PVNS   | Low signal intensity on T1- and T2-weighted MR images from hemosiderin deposition   |
| Rheumatoid arthritis                           | Uniform joint space narrowing, marginal erosions, pannus  |
| Infectious granulomatous diseases              |   |
| Tuberculous arthritis                          | Preserved joint spaces, marginal erosions, pannus, rice bodies  |
| Coccidioidomycosis arthritis                   | Preserved joint spaces, marginal erosions, pannus, rice bodies  |
| Deposition diseases                            |   |
| Gout   | Preserved joint spaces, overhanging edges, tophi  |
| Amyloid arthropathy                            | Preserved joint spaces, marginal erosions, juxtaarticular amyloid deposits with intermediate to low signal intensity on T1- and T2-weighted MR images |
| Vascular malformations                         |   |
| Synovial hemangioma                            | Lobulated mass with hyperintense signal on T2-weighted MR images, phleboliths   |
| AVM  | Flow voids in enlarged feeding arteries on MR images  |
| Malignancies                                   |   |
| Synovial chondrosarcoma                        | Lobulated mass with calcifications  |
| Synovial sarcoma                               | Calcifications, cystic areas, hemorrhage, fluid-fluid levels  |
| Synovial metastases                            | Nonspecific   |
| Miscellaneous                                  |   |
| Cyclops lesion                                 | Focal fibrous tumor in anterior joint space of knee, with intermediate to low signal intensity with all MR imaging pulse sequences                    |

25. Goldman AB, Bansal M. Amyloidosis and silicone synovitis: updated classification, updated pathophysiology, and synovial articular abnormalities. *Radiol Clin North Am* 1996; 34:375–394.
26. Quinton R, Siersema PD, Michiels JJ, ten Kate FJ, Renal AA. Amyloidosis in a patient with Bence Jones proteinuria and ankylosing spondylitis. *J Clin Pathol* 1992; 45:934–936.
27. Husby G. Amyloidosis. *Semin Arthritis Rheum* 1992; 22:67–82.
28. Sheldon PJ, Forrester DM. Imaging of amyloid arthropathy. *Semin Musculoskelet Radiol* 2003; 7:195–203.
29. Llauger J, Monill JM, Palmer J, Clotet M. Synovial hemangioma of the knee: MRI findings in two cases. *Skeletal Radiol* 1995; 24:579–581.
30. Greenspan A, Azouz EM, Matthews J 2nd, Decarie JC. Synovial hemangioma: imaging features in eight histologically proven cases, review of the literature, and differential diagnosis. *Skeletal Radiol* 1995; 24:583–590.
31. Price NJ, Cundy PJ. Synovial hemangioma of the knee. *J Pediatr Orthop* 1997; 17:74–77.
32. Choi JJ, Murphey MD. Angiomatous skeletal lesions. *Semin Musculoskelet Radiol* 2000; 4:103–112.
33. Dogan R, Dogan O, Oc M, Akata D, Gumus B, Balkanci F. A rare vascular malformation, Klippel-Trenaunay syndrome: report of a case with deep vein agenesis and review of the literature. *J Cardiovasc Surg (Torino)* 2003; 44:95–100.
34. Taconis WK, van der Heul RO, Taminiau AM. Synovial chondrosarcoma: report of a case and review of the literature. *Skeletal Radiol* 1997; 26:682–685.
35. Hermann G, Klein MJ, Abdelwahab IF, Kenan S. Synovial chondrosarcoma arising in synovial chondromatosis of the right hip. *Skeletal Radiol* 1997; 26:366–369.
36. Jones BC, Sundaram M, Kransdorf MJ. Synovial sarcoma: MR imaging findings in 34 patients. *AJR Am J Roentgenol* 1993; 161:827–830.
37. McCarville MB, Spunt SL, Skapek SX, Pappo AS. Synovial sarcoma in pediatric patients. *AJR Am J Roentgenol* 2002; 179:797–801.
38. Thompson KS, Reyes CV, Jensen J, Gattuso P, Sacks R. Synovial metastasis: diagnosis by fine-needle aspiration cytologic investigation. *Diagn Cytopathol* 1996; 15:334–337.
39. Laorr A, Helms CA. Cyclops lesion. In: Laorr A, Helms CA, eds. *MRI of musculoskeletal masses: a practical text and atlas*. New York, NY: Igaku-Shoin, 1997; 351–352.
40. Recht MP, Piraino DW, Cohen MA, Parker RD, Bergfeld JA. Localized anterior arthrofibrosis (cyclops lesion) after reconstruction of the anterior cruciate ligament: MR imaging findings. *AJR Am J Roentgenol* 1995; 165:383–385.